Inelastic and deep inelastic neutron spectroscopy of water molecules under ultra-confinement

IOP Conf. Series: Journal of Physics: Conf. Series **1055** (2018) 012002 doi:10.1088/1742-6596/1055/1/012002

Inelastic and deep inelastic neutron spectroscopy of water molecules under ultra-confinement

A I Kolesnikov[1,*], G F Reiter[2], T R Prisk[3], M Krzystyniak[4], G Romanelli[4], D J Wesolowski[5,#], and L M Anovitz[5]

[1]Neutron Scattering Division, Oak Ridge National Laboratory, Oak Ridge, Tennessee 37831, USA

[2]Physics Department, University of Houston, Houston, Texas 77204, USA

[3]Center for Neutron Research, National Institute of Standards and Technology, Gaithersburg, Maryland 20899-6100, USA

[4]ISIS Facility, Rutherford Appleton Laboratory, Chilton, Didcot, Oxfordshire OX11 0QX, UK

[5]Chemical Sciences Division, Oak Ridge National Laboratory, Oak Ridge, Tennessee 37831, USA

[*]Corresponding author: kolesnikovai@ornl.gov
[#]Retired from Chemical Sciences Division ORNL

Abstract. Water confined within sub-nanometer channels of silicate minerals presents an extreme case of confinement, where the restricted molecules are situated in channels whose diameter is not much larger than the water molecule itself. Recently, we discovered a new quantum tunneling state of the water molecule confined in 5 Å channels in the mineral beryl, characterized by extended proton and electron delocalization. Several peaks were observed in the inelastic neutron scattering (INS) spectra which were uniquely assigned to water quantum tunnelling. In addition, the water proton momentum distribution measured with deep inelastic neutron scattering (DINS) at 4.3 K directly showed coherent delocalization of the water protons in the ground state. The obtained average kinetic energy (E_K) of the water protons was found to be ~30% less than it is in bulk liquid water and ice phases. In the current work we present INS and DINS study of water in single crystal beryl in wider temperature range, T=5−260 K, where we observed significant increase of E_K of the confined water protons with temperature increase. The obtained INS data also indicate that with increasing temperature water molecules are progressively involved in hydrogen bonding (HB) with the beryl cage, while HB is almost absent at low temperatures.

1. Introduction

Water has many unusual properties in bulk states and under confinement [1-8]. The behavior of water confined within the nanopores with very weak water to pore surface interaction presents special interest because the reduced dimensionality could result in new phenomena, e.g. anomalously soft dynamics of water in quasi one-dimensional single-wall carbon nanotubes (SWNT) [9-12]. There are extreme cases when water is confined within the pores of a few Angstrom size, which can accommodate only one water molecule, such as water incapsulated in C_{60}-fullerenes [13], or water in mineral beryl [14]. Due to weak interaction with the walls, the confined water displays significant quantum behavior. In case of fullerenes water is almost free and quantum transitions between the para and ortho states of water in C_{60}-fullerenes were observed in inelastic neutron scattering (INS) experiments [15, 16], and quantum tunneling of water was suggested to explain the fine structure of the optical spectra of beryl [17-19]. Recently, using INS, deep inelastic neutron scattering (DINS) and *ab initio* calculations we discovered new quantum tunneling state of water in beryl, characterized by extended proton and electron delocalization [20]. The observed number of peaks in the INS spectra were uniquely assigned to water quantum tunneling, and the DINS study directly revealed that in the ground state water protons are coherently delocalized and have anomalously small average kinetic energy, E_K.

In the current work we present results of INS and DINS study of water in single crystal beryl in wide temperature range, T=5−260 K, to understand the vibrational dynamics of the water at higher temperatures, when all split ground states of water protons are well populated. We show that at high temperatures E_K of the water protons significantly increases (due to observed broadening of the proton momentum distribution).

2. Experimental

In this study we used low-alkali beryl single crystals (~0.1 wt.% of Na, see ref. 21 for details). The beryl structure ($Be_3Al_2Si_6O_{18}$, space group *P6/mcc*) consists of six-membered rings SiO_4 tetrahedra with open channels along the *c*-axis [14]. The channels form cavities 5.1 Å in diameter (which may contain alkali cations and water) separated by narrow (~2.8 Å) "bottlenecks". In alkali-poor beryl the water dipole moment is in the *ab*-plane and water protons are distributed over 6-fold equivalent positions across the channel, above and below the oxygen site. The used samples contain 0.6 water molecules per beryl formula unit, or about 2 wt.% water. Neutron spectroscopy is a preferred technique to study dynamics of the hydrogen containing materials, because neutron scattering cross-section for hydrogen (~82 barn for thermal neutrons, see [22]) is much larger than for other atoms, particularly this is right for beryl (7.63, 1.503, 2.167 and 4.232 barn for Be, Al, Si and O atoms, respectively), and INS can measure all vibrational modes.

2.1. Inelastic neutron scattering

The INS measurements were performed using the fine-resolution Fermi chopper spectrometer SEQUOIA at the Spallation Neutron Source at the Oak Ridge National Laboratory [23, 24]. To observe all possible vibrations with a good energy resolution ($\Delta E/E \approx$ 1-2% in the energy range of interest) we used five incident neutron energies, E_i=25, 50, 160, 250 and 800 meV. The measurements were conducted for two sample orientations, with neutron momentum transfer **Q** approximately parallel and perpendicular to the beryl crystal *c*-axis (see details in refs. [21, 25]). Most of the data were collected at seven temperatures, T=5, 25, 45, 80, 120, 200 and 260 K, which were controlled by closed-cycle helium refrigerator. The INS spectra from the empty container at the similar conditions were also measured and subtracted from the sample data. The collected INS data were corrected for the detectors efficiency and transformed from the time-of-flight and instrument coordinates to the dynamic structure factor *S(Q,E)* by using the MANTID [26] and DAVE [27] software packages.

2.2. Deep inelastic neutron scattering

The DINS (also known as Neutron Compton scattering) measurements [28, 29] were done using the VESUVIO spectrometer [30] at the ISIS pulsed neutron source. VESUVIO is an inverse-geometry

machine based on neutron capture resonances and its technical details can be found in [30, 31]. In the current experiment, we use 64 detectors, arranged with scattering angles from 37 to 67 on both sides of the beam. The data are corrected for multiple scattering [32] and a γ-ray background [33].

3. Results and discussion

3.1. Vibrational spectra and tunnelling modes

Figures 1 to 4 show the INS spectra for water in beryl at different temperatures. We used in this study different single crystals of beryl than in our previous work [20], but the results are well reproduced. The spectrum obtained at 5 K with E_i=25 meV (which provides good energy resolution data for energy transfer in the range 2 to 22 meV) for orientation **Q**⊥*c*-axis shows strong peaks at 8.4, 12.7 and 14.7 meV, which significantly decrease their intensities on heating to 25 K, and become invisible at higher temperatures. These peaks in the INS spectrum were assigned [20] to be due to the transitions between the lower and upper split ground state of water due to water tunneling between the six symmetrically equivalent positions around the *c*-axis in the channels of the beryl. This is understandable, because with temperature increase the lower ground state is depopulated due to transition to the higher split ground state according to Boltzmann law. The spectra for the orientation **Q**||*c*-axis show only one strong peak at around ~11 meV, which can be assigned to translational vibrations of water molecules along the *c*-axis. This peak is well observed up to the highest temperature 260 K. What is interesting, the position of the peak shows almost linear blue shift with temperature, from 10.9 meV at 5 K to 11.7 meV at 260 K. The peak width (full width at half maximum) also increases linearly from 0.71 meV at 5 K to 1.53 meV at 260 K. The large shift (7.3%) of the peak position to higher energy can be explained by negative thermal expansion of the beryl along the *c*-axis at temperatures below 600 K observed in previous x-ray diffraction results [34]. At room temperature the thermal expansion of beryl is $+2.6\cdot10^{-6}$ K^{-1} and $-2.9\cdot10^{-6}$ K^{-1} along the *a*- and *c*-axis, respectively, which is consistent with the values obtained in other studies [35, 36]. With temperature increase the intensity of this peak first increases (due to increase of Bose population factor) and then decreases (at T>150 K) due to suppression by the Debye-Waller factor, which we discussed in [20].

The spectra measured with E_i=50 meV (Figure 2, left panel) show a prominent band between 18 and 28 meV with two maxima at 21 and 24.5 meV for both orientations, with intensity of the band for **Q**⊥*c*-axis being about 1.6 times larger. We attribute this band to librational motions of the ultra-confined water molecules. This is consistent with the pioneering INS investigations of beryl [37], Raman spectroscopy studies [38], and first-principles calculations [39]. The band observed between 36 and 55 meV (Figure 2) is probably due to two-phonon neutron scattering involving the librational band at 18-28 meV. Other peaks are observed at 85, 96 and 151 meV for **Q**⊥*c*-axis orientation, and at 86, 114 and 128 meV for **Q**||*c*-axis (see Figure 2, right panel and Figure 3). The intensities of these phonon modes change a little with temperature increase from 5 to 260 K, and can be assigned to beryl cage vibrations [40], Al-O (85-86 meV), Be-O (96 meV) and Si-O (114, 127, 151 meV).

The peak at 197.5 meV is strong for **Q**||*c*-axis and very weak for **Q**⊥*c*-axis orientation (see Figure 3), and this peak can be assigned to water intramolecular bending H-O-H mode [20, 21], as we described in our previous study, in agreement with numerous literature data [17-19, 38-40]. The peaks at about 208.5, 219.3 and 230.1 meV can be well described as combination of the bending mode and the translational vibrations of water molecule along the *c*-axis (at 10.9 meV at 5 K).

The water intramolecular stretching O-H modes are observed at ~465 meV as strong and weak peaks for **Q**||*c*-axis and **Q**⊥*c*-axis orientations, respectively (see Figure 4). The obtained very large energy for the intramolecular stretching modes, and small value for the intramolecular bending mode (which are almost the same as for free water molecule) are in agreement with the assumption of absence of hydrogen bonds acting on water molecules in beryl, in accord with previous studies [17-19, 38-40]. The intensity of the peak at 465 meV for **Q**⊥*c*-axis orientation is much smaller than it should be based only on the

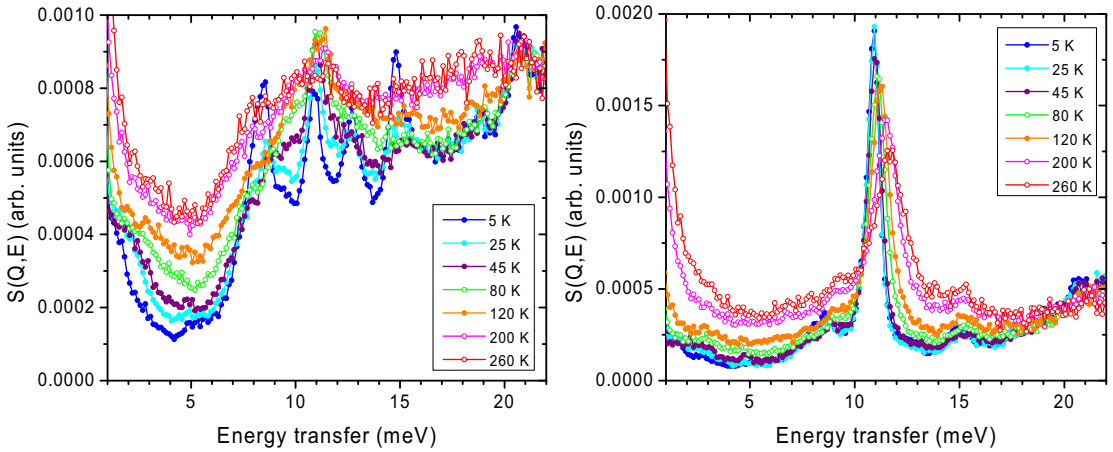

Figure 1. INS spectra of water in single crystal beryl at different temperatures, 5 to 260 K, measured with E_i=25 meV for neutron momentum transfer being approximately perpendicular and parallel to the crystal *c*-axis (left and right panels, respectively).

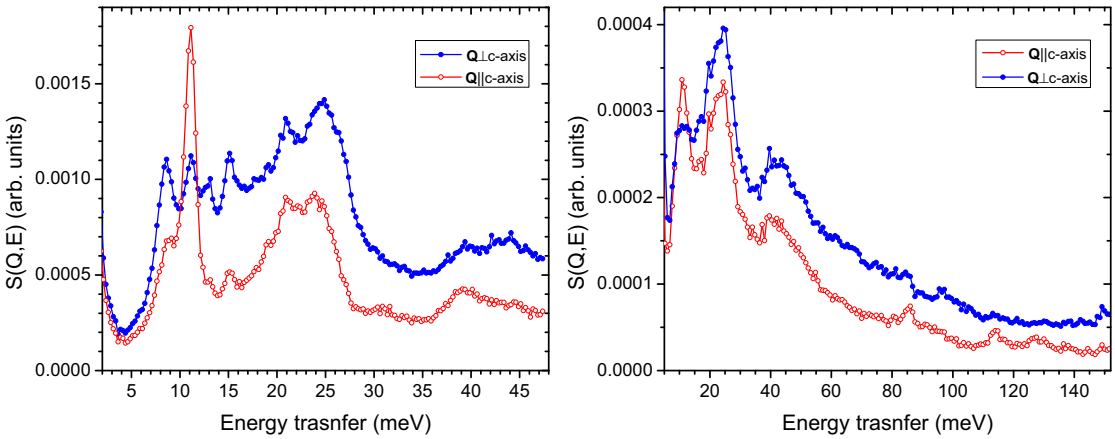

Figue 2. INS spectra of water in single crystal beryl at 5 K, measured with E_i=50 meV and 160 meV (left and right panels, respectively)

projections of the hydrogen displacement due to the stretching modes on the *ab*-plane and along *c*-axis, therefore an additional suppression of the peak should be involved due to the Debye-Waller factor, $DW=exp[-<(\mathbf{u}_H\mathbf{Q})^2>]$, where $\mathbf{u}_H$ is vibrational displacement of water protons. Hence, the data suggest larger mean squared displacement (MSD) of water protons in *ab*-plane. With temperature increase, the maximum value of the peak decreases (due to increase of the MSD of water protons), and a prominent excess of intensity is observed at the left side of the peak, between 405-440 meV. One might be tempted to attribute the increase in intensity on the left-hand side of the peak to multiphonon neutron scattering. Here the multiphonon process would consist of the simultaneous creation an O-H stretching mode quantum and the annihilation of low energy (translational and/or librational) water quanta. However, in that scenario, the effect would be proportional to the Bose population factor governing the low energy modes, $n(E_{LE},T)$. This implies that there should be an accompanying even larger increase in the scattering on the high-energy side of the peak, proportional to $n(E_{LE},T)+1$, which is inconsistent with the

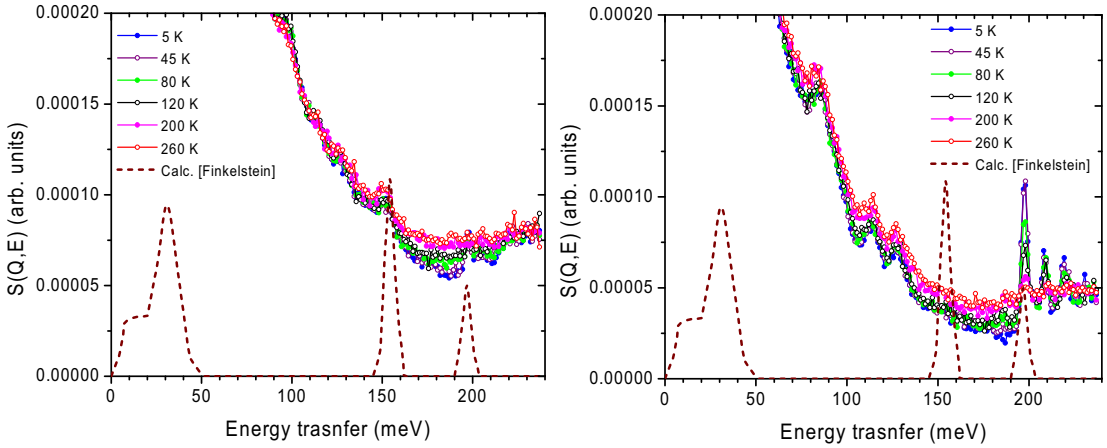

Figure 3. INS spectra of water in single crystal beryl at different temperatures, 5 to 260 K, measured with E_i=250 meV for neutron momentum transfer being approximately perpendicular and parallel to the crystal *c*-axis (left and right panels, respectively). Dashed lines show the calculated spectrum from [45].

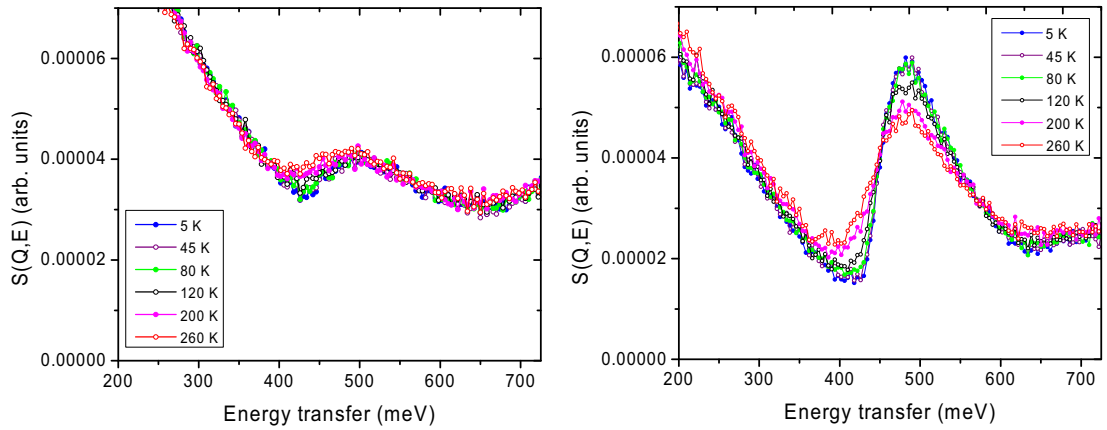

Figure 4. INS spectra of water in single crystal beryl at different temperatures, 5 to 260 K, measured with E_i=600 meV for neutron momentum transfer being approximately perpendicular and parallel to the crystal *c*-axis (left and right panels, respectively).

observed behavior. Rather, the additional intensity on the low energy side of the O-H stretching peak indicates significant softening of the stretching modes for at least some of the water molecules at higher temperatures (already at 120 K and above). Such softening is likely due to hydrogen bonding between the water molecules and the beryl cage.

This result sheds light on a discrepancy in our previous study [21] between the low temperature INS data, which suggested that no hydrogen bonding is present, and the high temperature (T=233-363 K) dielectric spectroscopic (DS) results, which proposed the presence of hydrogen bonds for water in beryl. Therefore, based on the INS and DS [21] results we propose that water in beryl does not form hydrogen bonds at low temperatures, and the hydrogen bonds progressively appear for some water molecules at higher temperatures.

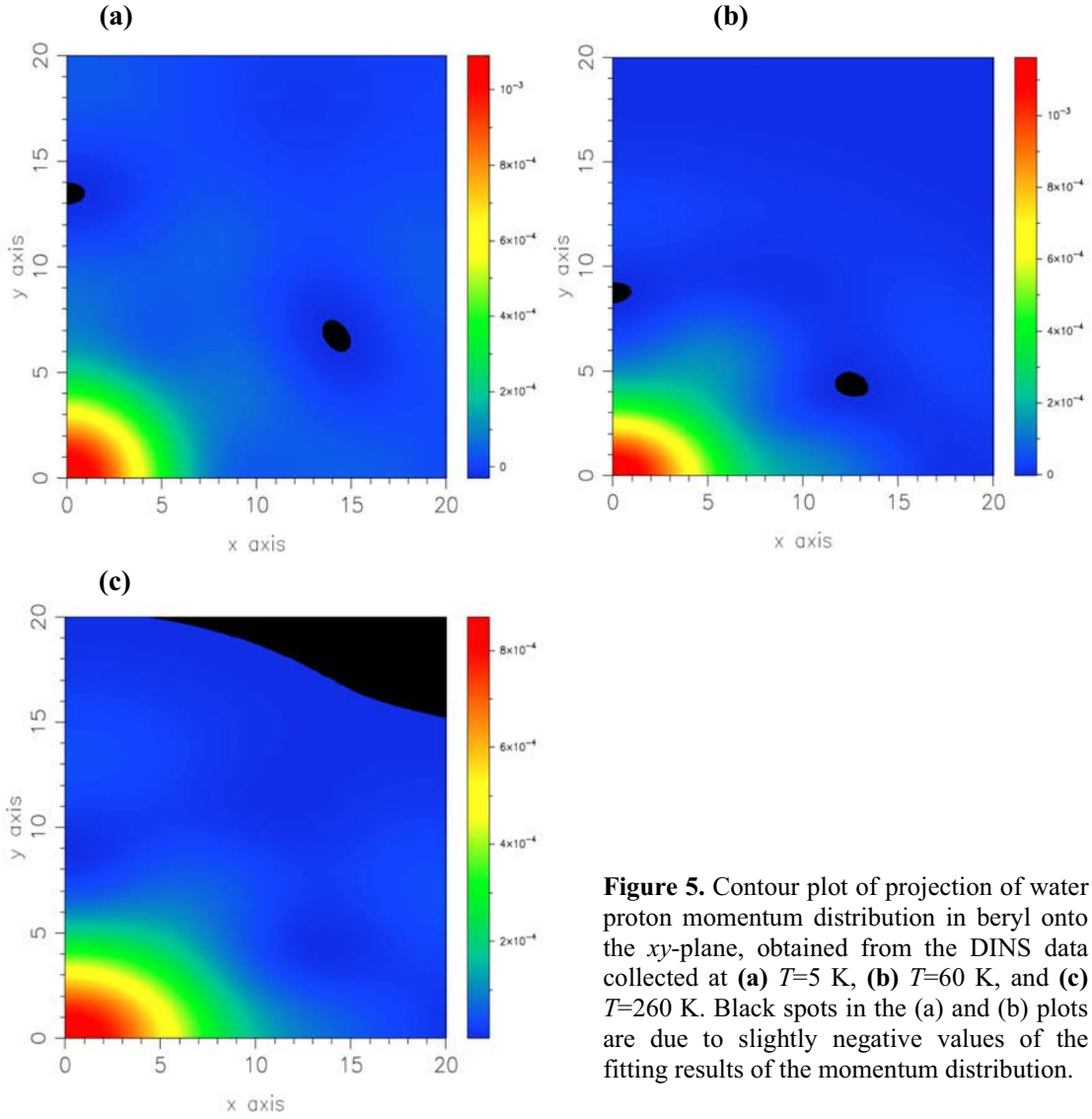

Figure 5. Contour plot of projection of water proton momentum distribution in beryl onto the *xy*-plane, obtained from the DINS data collected at **(a)** T=5 K, **(b)** T=60 K, and **(c)** T=260 K. Black spots in the (a) and (b) plots are due to slightly negative values of the fitting results of the momentum distribution.

3.2. Water protons momentum distribution and kinetic energy

The DINS spectra for beryl were collected for two orientations of beryl singles crystals, with their *c*-axis being vertical (perpendicular to the incoming neutron beam), and with *c*-axis being aligned along the incoming neutron beam. The data were treated with the use of MANTID software package [41]. The data for both configurations were fitted simultaneously to a 3D momentum distribution that is the average distribution of the two protons of the water molecule. We used a basis of Hermite polynomials of tenths order (with the terms consistent with the sixfold symmetry of the beryl channel) and spherical harmonics [12]. The *z*-axis of the fitting was chosen along the crystal *c*-axis, and the *xy*-plane was perpendicular to *z*-axis (parallel to the *ab*-plane). Figure 5 shows the contour plots of projection of water proton momentum distribution in beryl onto the *xy*-plane at different temperatures, and Figure 6 shows the curves fitted to the measured Compton profiles along the *x*-, *y*- and *z*-axis, and the corresponding parameters σ_x, σ_y and σ_z, that determine the width of the momentum distribution along the corresponding

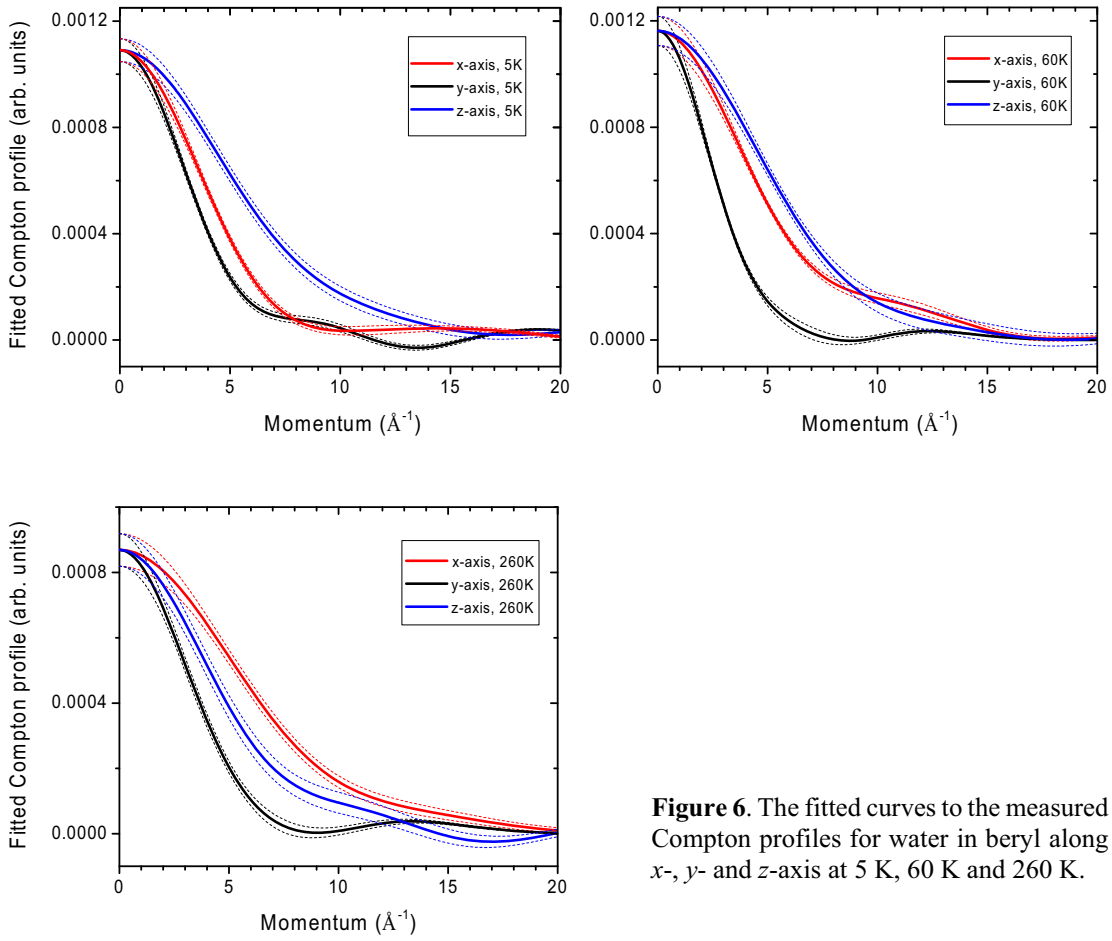

Figure 6. The fitted curves to the measured Compton profiles for water in beryl along *x*-, *y*- and *z*-axis at 5 K, 60 K and 260 K.

axis, are presented in Table 1. We notice that the fitting results in Figures 5 and 6 show slightly negative values of the momentum distribution. It can be extremely difficult to impose non-negativity constraints on the intensity of the momentum distribution when several Hermite polynomials are considered. As non-constrained coefficients can affect the value of the mean kinetic energy, one should pay attention to such aspect. In this light, the article by Krzystyniak in these proceedings [42] discusses the analytic constraints amongst the fitting parameters in the case of polynomials up to the fourth order. In our results, the slight negativity of the momentum distribution could be justified by including the fitting error bars, therefore making the result overall compatible with the non-negativity constraints.

The average kinetic energy of proton E_K is proportional to the second moment of momentum distribution and can be expressed as:

$$E_K = \frac{\hbar^2}{2m}(\sigma_x^2 + \sigma_y^2 + \sigma_z^2), \quad (1)$$

where m is mass of proton. The obtained E_K are 104.0 meV, 207.7 meV and 210.3 meV for 5, 60 and 260 K, respectively. The widths of momentum distribution E_K at 5 K is in very good agreement with our old data at 4.3 K measured on different beryl sample. We anticipated increase of average kinetic energy of water proton at higher temperatures due to occupation not only the lower split ground state (as at 5K) but also other split ground states, which should result in broadening of the momentum distribution. The

Table 1. The widths ($Å^{-1}$) of momentum distribution for water proton in beryl.

Temperature, K	σ_x	σ_y	σ_z
4.3 (ref. [20])	3.66	3.61	4.98
5	4.13	3.40	4.65
60	5.83	3.51	7.35
260	6.77	3.90	6.37

observed two times increase of E_K already at 60 K is very unusual, but so large values for proton kinetic energy were documented before for water confined in double wall carbon nanotubes of 16 Å inner diameter (198 meV at 120 K, and 221 meV at 170 K), in Nafion-1120* (245 meV at 300 K), and Dow-858* (262 meV at 300 K) [43]. So, at low temperature (5 K) water in beryl shows coherent quantum delocalization (tunneling) over six equivalent positions across the channel, and water protons are localized in inverse (momentum) space, having narrow momentum distribution and low average kinetic energy. With temperature increase, water still tunnel between these positions, and it progressively occupies other split ground states, which results in increase of E_K.

In the semi-empirical (SE) harmonic approximation (see e.g. [44]) due to very large values of the O-H stretching modes of water in beryl (~465 meV) the estimated E_K, with the use of only water intramolecular modes, should be 132.5 meV [20, 44]. The measured energy of the stretching modes is the energy difference between the first excited and ground states, and the energy of the ground state is assumed to be half of this difference. Probably, the energy of the ground state of the tunneling particle is much lower than that for particle in single harmonic potential.

Recently, DFT based first-principles calculations were carried out for beryl [45], where the obtained generalized vibrational density of states (GVDOS) for water protons (shown as dashed lines in the Figure 3) well describes our INS spectra: the intramolecular stretching and bending modes are in excellent agreement with the experiment. The authors [45] did not make assignments for the low-energy modes, but the part of the spectrum below 20 meV could be probably related to the water translational modes (there is a peak in this range of GVDOS for oxygen atoms, which are mostly involved in the translational vibrations of water), therefore the peak around 30 meV should be due to water librational vibrations, which is in accord with INS data. The calculated (high intensity) peak at 154 meV is the only one, which does not correspond to the peak from water protons in the measured spectrum. There is actually a peak in the INS data (obtained for $\mathbf{Q}\perp c$-axis orientation) but the temperature dependence of the intensity of the peak and other literature data indicate that this peak is due to vibrations of beryl cage, as discussed above. Using the DFT derived GVDOS for water proton the authors [45] calculated the mean kinetic energy (E_K=104.4 meV) which is in remarkable agreement with the 5 K DINS data. The big discrepancy between the new calculated value and the old one, estimate in SE approach, was explained by different distribution of GVDOS of protons, most probably due to coupling with vibrational modes of the beryl cage. We think that, unfortunately, there is a mistake in the calculated GVDOS for water in beryl. From the values of energy fractions shared by the H and O atoms in beryl presented in Table VI of the ref. [45], it follows violation of one from two known sum rules, which are known as "the orthonormality and closure conditions" (see e.g. [46]):

$$\sum_{i=1}^{3}|\mathbf{e}(i|\mathbf{k}j)|^2 = 1 \quad (2)$$

and

$$\sum_{j=1}^{9}|\mathbf{e}(i|\mathbf{k}j)|^2 = 1, \quad (3)$$

where i is the atomic number in the primitive cell (i=1 to 3, for 2 hydrogen atoms and 1 oxygen), $\boldsymbol{k}$ is a wave vector, and j stands for phonon branches (j=1 to 9, for 3 translational, 3 librational and 3 intramolecular modes for H_2O). The squared phonon eigenvectors in the above equations directly relate to energy fractions used in [45]. The Eq. (3) is well satisfied, while the Eq. (2) is not: the sum over all atoms is about twice larger for the lowest energy mode, and the sum is twice smaller for intramolecular modes, than they should be. The proposed explanation [45] that this (very large) violation is due to

coupling of the water intramolecular vibrations with the hosting beryl nano-cage does not look acceptable because in this case the energy of the intramolecular modes should be strongly changed, while they almost coincide to those for the free water molecule (with no HB). Therefore, the very low average kinetic energy of water protons in beryl at 5 K obtained from the DINS data is still awaiting a quantitative explanation.

4. Conclusion

We studied dynamics of single crystal beryl in wide temperature range, from 5 to 260 K, by using INS and DINS technique. The obtained data confirm our previous study [20] that at 5 K water molecule exhibits quantum tunneling behavior, and protons have very small average kinetic energy (104 meV). At 60 K, and also at 260 K, the E_K increases about two times. In the INS spectra we observed also appearing of the low energy feature of the water O-H stretching peak with temperature increase (at 120 K and above) which indicates progressive appearance of the hydrogen bonding of some water molecules with the beryl cage.

Acknowledgements

The neutron scattering experiment at Oak Ridge National Laboratory's Spallation Neutron Source was sponsored by the Scientific User Facilities Division, Office of Basic Energy Sciences, U.S. Department of Energy. This research was sponsored by the Division of Chemical Sciences, Geosciences, and Biosciences, Office of Basic Energy Sciences, U.S. Department of Energy. The STFC Rutherford Appleton Laboratory is thanked for access to neutron beam facilities. Some of the beryl crystals used in our experiments were cut by Bradley S. Wilson of Coast-to-Coast Rarestones, International.

References

[1] Ball P 2008 Water–An enduring mystery *Nature* **452** 291
[2] Finney J L 2004 Water? What's so special about it? *Phil. Trans. R. Soc. B* **359** 1145
[3] Angell C A 2008 Insights into phases of liquid water from study of its unusual glass-forming properties *Science* **319** 582
[4] Debenedetti P G and Stanley H E 2003 Supercooled and glassy water *Phys. Today* **56** 40
[5] Wang H-W, DelloStritto M J, Kumar N, Kolesnikov A I, Kent P R C, Kubicki J D, Wesolowski D J, and Sofo J O 2014 Vibrational density of states of strongly H-bonded interfacial water: Insights from inelastic neutron scattering and theory *J. Phys. Chem. C* **118** 10805
[6] Gainaru C, Agapov A L, Fuentes-Landete V, Amann-Winkel K, Nelson H, Köster K, Kolesnikov A I, Novikov V N, Richert R, Böhmer R, Loerting T, and Sokolov A P 2014 Anomalously large isotope effect in the glass transition of water *Proc. Natl. Acad. Sci.* **111** 17402-17407
[7] Reiter G F, Deb A, Sakurai Y, Itou M, Krishnan V G, and Paddison S J 2013 Anomalous ground state of the electrons in nanoconfined water *Phys. Rev. Lett*. **111** 036803
[8] Algara-Siller G, Lehtinen O, Wang F C, Nair R R, Kaiser U, Wu H A, Geim A K, and Grigorieva I V 2015 Square ice in graphene nanocapillaries *Nature* **519** 443
[9] Hummer G, Rasaiah J C, and Noworyta J P 2001 Water conduction through the hydrophobic channel of a carbon nanotube *Nature* **414** 188-190
[10] Koga K, Gao G T, Tanaka H, and Zeng X C 2001 Formation of ordered ice nanotubes inside

carbon nanotubes *Nature* **412** 188-190
[11] Kolesnikov A I, Zanotti J-M, Loong C-K, Thiyagarajan P, Moravsky A P, Loutfy R O, and Burnham C J 2004 Anomalously soft dynamics of water in a nanotube: a revelation of nanoscale confinement *Phys. Rev. Lett.* **93** 035503
[12] Reiter G, Burnham C, Homouz D, Platzman P M, Mayers J, Abdul-Redah T, Moravsky A P, Li J C, Loong C-K, and Kolesnikov A I 2006 Anomalous zero point motion of the protons in water in carbon nanotubes *Phys. Rev. Lett.* **97** 247801
[13] Kurotobi K and Murata Y 2011 A single molecule of water encapsulated in fullerene C_{60} *Science* **333** 613
[14] Diego Gatta G, Nestola F, Bromiley G D, and Mattauch S 2006 The real topological configuration of the extra-framework content in alkali-poor beryl: A multi-methodological study *Am. Mineral.* **91** 29
[15] Beduz C, Carravetta M, Chen J Y-C, Concistrè M, Denning M, Frunzi M, Horsewill A J, Johannessen O G, Lawler R, Lei X, Levitt M H, Li Y, Mamone S, Murata Y, Nagel U, Nishida T, Ollivier J, Rols S, Rõõm T, Sarkar R, Turro N J, and Yang Y 2012 Quantum rotation of *ortho* and *para*-water encapsulated in a fullerene cage *Proc. Natl. Acad. Sci. U.S.A*. **109** 12894-12898
[16] Goh K S K, Jiménez-Ruiz M, Johnson M R, Rols S, Ollivier J, Denning M S, Mamone S, Levitt M H, Lei X, Li Y, Turro N J, Muratae Y, and Horsewill A J 2014 Symmetry-breaking in the endofullerene $H_2O@C_{60}$ revealed in the quantum dynamics of ortho and para-water: a neutron scattering investigation *Phys. Chem. Chem. Phys.* **16** 21330-21339
[17] Gorshunov B P, Zhukova E S, Torgashev V I, Lebedev V V, Shakurov G S, Kremer R K, Pestrjakov E V, Thomas V G, Fursenko D A, and Dressel M 2013 Quantum behavior of water molecules confined to nanocavities in gemstones *J. Phys. Chem. Lett*. **4** 2015-2020
[18] Gorshunov B P, Zhukova E S, Torgashev V I, Motovilova E A, Lebedev V V, Prokhorov A S, Shakurov G S, Kremer R K, Uskov V V, Pestrjakov E V, Thomas V G, Fursenko D A, Kadlec C, Kadlec F, and Dressel M 2014 THz-IR spectroscopy of single H_2O molecules confined in nanocage of beryl crystal lattice *Phase Transitions* **87** 966-972
[19] Zhukova E S, Torgashev V I, Gorshunov B P, Lebedev V V, Shakurov G S, Kremer R K, Pestrjakov E V, Thomas V G, Fursenko D A, Prokhorov A S, and Dressel M 2014 Vibrational states of a water molecule in a nano-cavity of beryl crystal lattice *J. Chem. Phys*. **140**, 224317
[20] Kolesnikov A I, Reiter G F, Choudhury N, Prisk T R, Mamontov E, Podlesnyak A, Ehlers G, Seel A, Wesolowski D J, and Anovitz L M 2016 Quantum tunneling of water in beryl: A new state of water molecule *Phys. Rev. Lett*. **116** 167802
[21] Anovitz L M, Mamontov E, ben Ishai P, and Kolesnikov A I 2013 Anisotropic dynamics of water ultra-confined in macroscopically oriented channels of single-crystal beryl: A multi-frequency analysis *Phys. Rev. E* **88** 052306
[22] Sears V F 1992 Neutron scattering lengths and cross sections *Neutron News* **3** 26-37
[23] Granroth G E, Kolesnikov A I, Sherline T E, Clancy J P, Ross K A, Ruff J P C, Gaulin B D, and Nagler S E 2010 SEQUOIA: a newly operating chopper spectrometer at the SNS *J. Phys.: Conf. Ser.* **251** 012058
[24] Stone M B, Niedziela J L, Abernathy D L, DeBeer-Schmitt L, Ehlers G, Garlea O, Granroth G E, Graves-Brook M, Kolesnikov A I, Podlesnyak A, and Winn B 2014 A comparison of four direct geometry time-of-fight spectrometers at the Spallation Neutron Source *Rev. Sci. Instrum.* **85** 045113
[25] Kolesnikov A I, Anovitz L M, Mamontov E, Podlesnyak A, and Ehlers G 2014 Strong anisotropic dynamics of ultra-confined water *J. Phys. Chem. B* **118** 13414-13419
[26] Arnold O *et al*. 2014 Mantid–data analysis and visualization package for neutron scattering and μSR experiments *Nucl. Instrum. Methods A* **764** 156-166
[27] Azuah R T, Kneller L R, Qiu Y, Tregenna-Piggott P L W, Brown C M, Copley J R D, and Dimeo R M 2009 DAVE: A comprehensive software suite for the reduction, visualization, and

analysis of low energy neutron spectroscopic data *J. Res. Natl. Inst. Stand. Technol*. **114** 341-358

[28] Andreani C, Colognesi D, Mayers J, Reiter G F, and Senesi R 2005 Measurement of momentum distribution of light atoms and molecules in condensed matter systems using inelastic neutron scattering *Adv. Phys.* **54** 377-469

[29] Andreani C, Krzystyniak M, Romanelli G, Senesi R, and Fernandez-Alonso F 2017 Electron-volt neutron spectroscopy: beyond fundamental systems *Adv. Phys.* **66** 1-73

[30] Mayers J and Adams M A 2011 Calibration of an electron volt neutron spectrometer *Nucl. Instrum. Methods A* **625** 47-56

[31] Romanelli G, Krzystyniak M, Senesi R, Raspino D, Boxall J, Pooley D, Moorby S, Schooneveld E, Rhodes N J, Andreani C, and Fernandez-Alonso F 2017 Characterisation of the incident beam and current diffraction capabilities on the VESUVIO spectrometer *Meas. Sci. Technol*. **28** 095501

[32] Mayers J, Fielding A, and Senesi R 2002 Multiple scattering in deep inelastic neutron scattering: Monte Carlo simulations and experiments at the ISIS eVS inverse geometry spectrometer *Nucl. Instrum. Methods A* **481** 454-463.

[33] Mayers J 2011 Calculation of background effects on the VESUVIO eV neutron spectrometer *Meas. Sci. Technol*. **22** 015903

[34] Morosin B 1971 Structure and thermal expansion of beryl *Acta Cryst*. **B28** 1899-1903

[35] Schlenker L, Gibbs G V, Hill E G, Crews S S, and Myers R H 1977 Thermal expansion coefficients for indialite, emerald, and beryl *Phys. Chem. Minerals* **1** 243-255

[36] Fan D, Xu J, Kuang Y, Li X, Li Y, and Xie H 2015 Compressibility and equation of state of beryl ($Be_3Al_2Si_6O_{18}$) by using a diamond anvil cell and in situ synchrotron X-ray diffraction *Phys. Chem. Minerals* **42** 529–539

[37] Boutin H, Prask H, and Safford G J 1965 Low frequency motions of H_2O molecules in beryl from neutron inelastic scattering data *J. Chem. Phys*. **42** 1469-1470

[38] Kolesov B A and Geiger C A 2000 The orientation and vibrational states of H_2O in synthetic alkali-free beryl *Phys. Chem. Minarals* **27** 557-564

[39] Belyanchikov M A, Zhukova E S, Tretiak S, Zhugayevych A, Dressel M, Uhlig F, Smiatek J, Fyta M, Thomas V G, and Gorshunov B P 2017 Vibrational states of nano-confined water molecules in beryl investigated by first-principles calculations and optical experiments *Phys. Chem. Chem. Phys.* **19** 30740

[40] Adams D M and Gardner I R 1974 Single-crystal vibrational spectra of beryl and dioptase *J. Chem. Soc., Dalton Trans*. **0** 1502-1505

[41] Jackson S, Krzystyniak M, Seel A G, Gigg M, Richards S E, and Fernandez-Alonso F 2014 VESUVIO data analysis goes MANTID *J. Phys.: Conf. Ser.* **571** 012009

[42] Krzystyniak M *et al*. 2018 Model selection in neutron Compton scattering – A Bayesian approach with physical constraints *J. Phys.: Conf. Ser.* (in this volume)

[43] Reiter G F, Kolesnikov A I, Paddison S J, Platzman P M, Moravsky A P, Adams M A, and Mayers J 2012 Evidence for an anomalous quantum state of protons in nanoconfined water *Phys Rev B* **85** 045403

[44] Finkelstein Y and Moreh R 2016 Proton dynamics in hydrogen-bonded systems *Mol. Phys.* **114** 2108-2114

[45] Finkelstein Y, Moreh R, Shang S L, Wang Y, and Liu Z K 2017 Quantum behavior of water nano-confined in beryl *J. Chem. Phys*. **146** 124307

[46] Born M and Huang K 1954 *Dynamical theory of crystal lattices* (Oxford: Clarendon Press)